Efficient rectifier with wide input power range for 5G applications

Mounira Ben Yamna[1], Nabil Dakhli[2], Hedi Sakli[1,3], Mohamed Aoun[1]

[1]MACS Laboratory, National Engineering School of Gabes, University of Gabes, Medenine, Tunisia
[2]Innov'COM Lab, Sup'COM, University of Carthage, Qart Hadasht, Tunisia
[3]EITA Consulting, Montesson, France

Article Info

ABSTRACT

This article presents three efficient rectifiers for radio frequency energy harvesting (RFEH) systems operating at the fifth generation (5G) band (3.5 GHz). Each rectifier operates at various input power levels (high, low, and across a wide power range). The high and low-power rectifiers feature a single serial topology using HSMS-2860 and SMS-7630 Schottky diodes, respectively, along with microstrip lines to implement the input and output filters and the impedance matching network. At an radio frequency (RF) power level of 15 dBm, the high-power rectifier harvests 67.4% to direct current (DC) power with a 300 Ω load resistor and an output voltage of 2.5 V. The low-power rectifier achieves its maximum power conversion efficiency (PCE) at -2 dBm, reaching 45% efficiency with a 1,200 Ω load. The rectifier with a extended input power range comprises two branches of subrectifiers functioning at both high and low power levels. Depending on the power level, the considered subrectifier harvests radio frequency power into DC power, while the other subrectifier is deactivated. Across a power span of 32.5 dB (ranging from -13 to 19.5 dBm), the rectifier maintains an efficiency above 30%. The proposed rectifiers are efficient and suitable for implementation in 5G-enabled RFEH systems.

Corresponding Author:

Mounira Ben Yamna
MACS laboratory, National Engineering School of Gabes, University of Gabes
B.P.132, Medenine, Tunisia
Email: benyemnamounira@gmail.com

1. INTRODUCTION

The growth of high data rate, high-speed data transmission, low power consumption, and reliable communication is giving rise to new wireless technologies such as the 5th generation (5G), mobile networks, and the internet of things (IoT). The frequency spectrum of 5G consists of three bands, with the most widely used band being the sub-6 GHz, covering from 450 MHz to 6 GHz [1]. The impressive development in the number of connected objects implies a massive deployment of sensors, necessitating the regular charging or changing of batteries. Consequently, the design of rechargeable autonomous devices will be a challenging task [2]. To address this issue, radio-frequency energy harvesting (RFEH) is being considered as the solution. The rectenna is the key element of RFEH systems, comprising a receiving antenna and a rectifying circuit [3]. The rectenna's performance depends on two main factors: the radio frequency (RF) input power captured by the antenna and its conversion to direct current (DC) power by the rectifier [4]. Classifying rectifiers is determined by the operational level of RF input power, categorizing them into low-power, high-power, and wide power

range devices. In the literature, various rectifiers at different power levels have been investigated for energy harvesting (EH) systems [5]-[9]. Its performance is evaluated by the power conversion efficiency (PCE) or the RF-DC efficiency. This efficiency is influenced by factors such as the Schottky diode type, input power level, input impedance, and operating frequency [10]. The ambient RF power in EH systems is inherently unpredictable, and the unexpected change of input power level has the potential to influence the input impedance of the rectifier due to its non-linearity [11]. This change results in an impedance mismatch between the receiving antenna and the rectifying circuit, leading to a decrease in the maximum energy transfer. This explains the difficulty in creating a rectifier capable of accommodating a extended range of RF input power. Several works have focused on stabilizing rectifier performance in response to fluctuations in operating conditions. To minimize the susceptibility of the rectifier circuit to radio frequency input power fluctuations, an impedance compression network (ICN) and a resistance compression network (RCN) are utilized in [12] and [13], respectively. The ICN circuit compresses the complex input impedance, while the RCN affects the real part of the input impedance. However, ICN and RCN circuits have limitations in certain impedance circumstances. In [14], two subrectifier cells operating at both low and high input power levels were associated using a T-junction power divider. In [15], three subrectifiers were combined utilizing a branch line coupler (BLC), with two functioning at a high power level and the third one at a low power level. To avoid insertion losses from extra devices (coupler, power divider), which can influence rectifier performance, an adaptive power distribution network was proposed in [16] and [17]. It comprises two subrectifiers working at both low and high input power levels. A gallium arsenide (GaAs) pseudomorphic high electron mobility transistor (pHEMT) with Schottky diode was used, in [18], to increase RF input power band by achieving a reduced threshold voltage and increased breakdown voltage. Additionally, to obtain a wide RF input power band, a power division diode array was utilized in [19]. The described works have been used for various input power levels (high, low and wide band) and employed various techniques to improve performance. These studies have also covered different frequency bands such as global system for mobile communication (GSM) (0.915 GHz) and wireless fidelity (WiFi) (2.45 GHz). The authors noted a lack of literature on rectifiers operating at 3.5 GHz with an extended input power band. In this submitted manuscript, a rectifier suitable for RFEH applications operating at sub-6 GHz (3.5 GHz) was studied and simulated. The novelty lies in the conception of a rectifier with a wide input power range operating at 3.5 GHz without the use of lumped elements. Microstrip lines technology was employed to design the impedance matching network (IMN) and filters, within which capacitive and inductive losses were minimized. The proposed rectifier designed to accommodate a extended input power range, comprises two branches of microstrip lines directly connected without extra devices, featuring a simple IMN. This design covers different power levels: low (less than 0 dBm) and high (greater than 0 dBm) across a span of 32.5 dB (ranging from -13 to 19.5 dBm).

The designs and simulated results of the rectifiers created for high power and low power are illustrated in sections 2 and 3, respectively. The power distribution technique applied to the extended input power band rectifier is elucidated in section 4. Ultimately, in section 5 a conclusion is discussed, then the references are cited at the end of the manuscript.

2. HIGH POWER RECTIFIER
2.1. The design description

To design an RF energy rectifying circuit functioning at a frequency of 3.5 GHz for a high RF input power band varying from 0 to 20 dBm, a simple serial rectifier is proposed. The chosen substrate is made of FR4 epoxy with a thickness (h) of 1.6 mm and dielectric properties ϵ=4.4, tanδ=0.02. The structure comprises an impedance matching network (IMN), a high frequency (HF) bandpass filter, a HSMS-2860 Schottky diode from Avago, a DC low pass filter, and a resistor load [20], as illustrated in Figure 1. The DC low pass filter is composed of four transmission lines (TL8, TL9, TL10, TL11) acting as parallel capacitors and serial inductors. It is inserted after the diode to allow only the DC signal to pass while blocking the fundamental and the harmonics [21]. The chosen Schottky diode is the HSMS-2860 with a junction voltage (V_j) set at 0.65 V and a breakdown voltage (V_{br}) established at 7 V, making it suitable for high-power rectification. The HF input filter is a band-pass filter positioned between the receiving antenna and the rectifier. It incorporates a $\lambda/4$ shorted length stub (TL5) to inhibit the return of harmonics produced by the diode [22]. Additionally, T-shaped transmission lines (TL1, TL2, TL3) are integrated to create a proper matching network, ensuring optimal power transmission with a load resistor of 300 Ω.
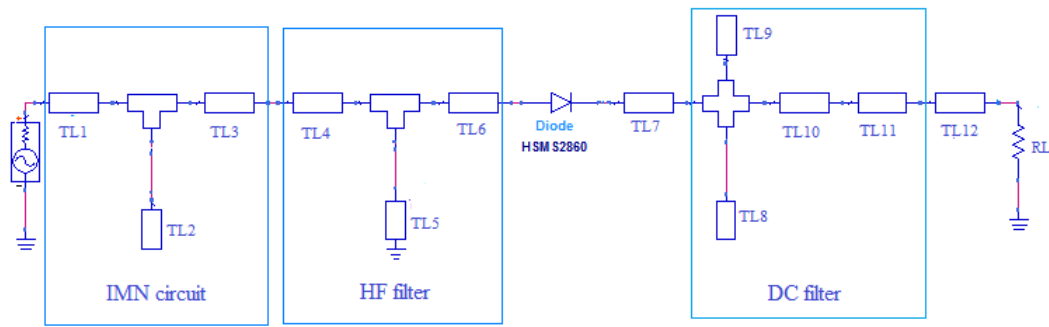
Figure 1. Schematic of the high power rectifier

The optimal dimensions of the transmission lines (TL) employed in the rectifier design are illustrated in Table 1. The primary goal of the rectifying circuit is to achieve RF-to-DC conversion with utmost efficiency. The power conversion efficiency (PCE) is defined as (1). The relationship between DC output power (P_{DC}) and RF input power (P_{in}).

$$PCE(\%) = \frac{P_{DC}}{P_{in}} \times 100 \tag{1}$$

Table 1. Dimensions of the transmission lines forming the high power rectifier

TL	Width (mm)	Length (mm)
TL1	5	1.5
TL2	3	6
TL3	2.9	2
TL4	3	3
TL5	3	11
TL6	3	5.1
TL7	3	2.9
TL8	3	12
TL9	3	5
TL10	3	3
TL11	17.3	11.5
TL12	3	3

2.2. Simulation results

To boost the high-power rectifier's performance, PCE is measured at 3.5 GHz for various load and input power level settings. The rectifier simulation results are obtained using keysight advanced design system (ADS) software, depicting parameters like the reflection coefficient S_{11} vs. frequency and PCE vs. input power (P_{in}) in Figure 2. A large signal S-parameter (LSSP) solver is employed to visualize the matching behavior of the rectifying circuit at different values of P_{in}. The reflection coefficient reaches -25 dB at 3.5 GHz as illustrated in Figure 2(a), indicating good matching, the rectifier exhibits good matching in the frequency range of 3.3 to 3.85 GHz at an input power of 15 dBm. To determine a suitable load, PCE vs. P_{in} is examined for different values of load R_L as illustrated in Figure 2(b) using the harmonic balance (HB) solver of ADS. The maximum achieved PCE is 67.4% at 3.5 GHz for a 300 Ω resistor and an RF input power level of 15 dBm. As visualized in Figure 2(c), the output voltage is 2.5 V.

3. LOW POWER RECTIFIER
3.1. The design description

Considering the level of input power, the Schottky diode is selected. Equation (2) suggests that the maximum power-handling capacity is dependent on the breakdown voltage (V_{br}) and the load resistor (R_L) [23].

$$P_{out}(max) = \frac{V_{br}^2}{4 \times R_L} \tag{2}$$

For power levels higher than $P_{out}(max)$, the rectifying circuit will cease to harvest the RF power. Therefore, a Schottky diode with a low breakdown voltage and a high R_L is more suitable for a low-power rectifier. For this reason, the SMS-7630 diode from Skyworks with V_{br}=2 V is chosen to design the low-power rectifier, with a load resistor of 1200 Ω. The designed harvester is depicted in Figure 3, where only the Schottky diode, the load, and the IMN circuit differ from those of the first rectifier described in section 2. Dimensions of the matching network transmission lines are illustrated in Table 2.

(a)

(b)

(c)
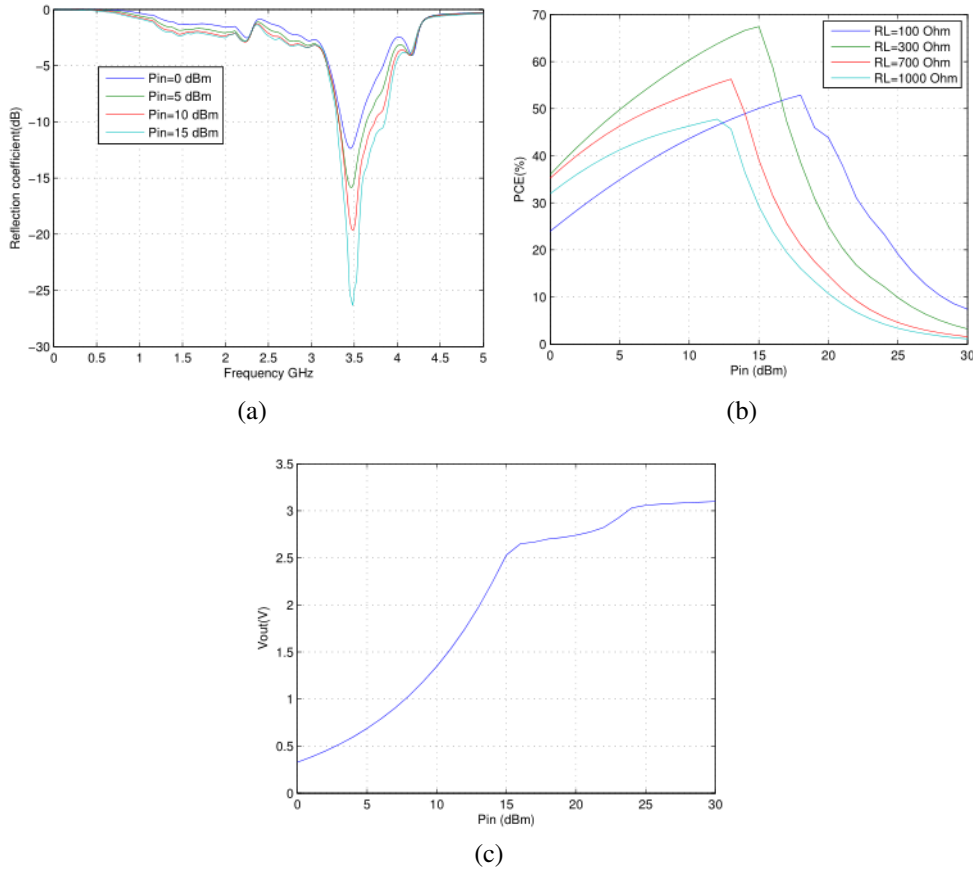
Figure 2. Comparison simulation results (a) reflection coefficient vs. frequency and (b) PCE vs. P_{in} (c) V_{out} vs. P_{in}
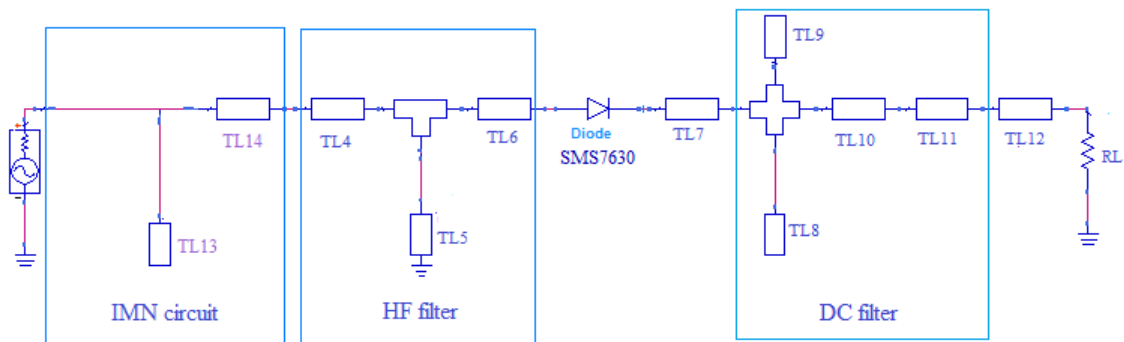
Figure 3. Schematic of the low power rectifier

Table 2. Dimensions of the transmission lines forming the low power rectifier

TL	Width (mm)	Length (mm)
TL13	2	20.2
TL14	3	26

3.2. Simulation results

The designed low-power rectifier is analyzed using harmonic balance (HB) and LSSP solvers of ADS software. The simulated reflection coefficient S_{11} vs. frequency at P_{in}=-10, -5, and 0 dBm is shown in Figure 4(a). It reaches -20 dBm at 3.5 GHz for an RF input power of -10 dBm. Also, simulated PCE vs. P_{in} is shown in Figure 4(b), where the maximum PCE is equal to 45% at -2 dBm. The simulated V_{out} vs. frequency at various values of P_{in} is depicted in Figure 4(c). The maximum value reaches 0.7 V at 0 dBm.

(a)

(b)

(c)
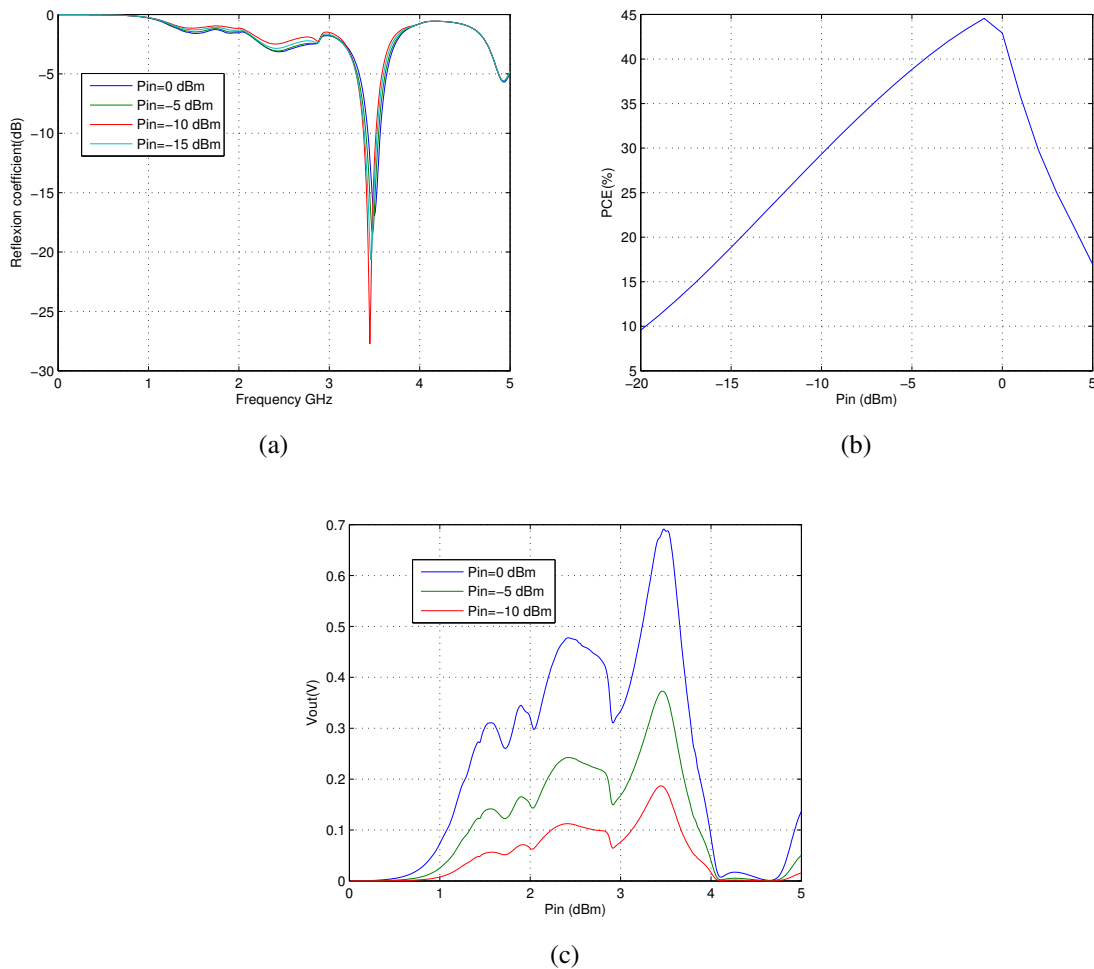
Figure 4. Comparison simulation results (a) reflection coefficient vs. frequency and (b) PCE vs. P_{in} (c) V_{out} vs. frequency

4.   WIDE INPUT POWER RANGE RECTIFIER
4.1. Design description

In this section, a novel rectifier with a wide RF input power range is designed in Figure 5. It comprises two subrectifiers, A and B, in parallel, directly linked to the input port without the need for extra devices, operating at both low and high power levels, respectively. This innovative design enables efficient energy harvesting across a broad range of input power levels, utilizing a special distribution power technique.
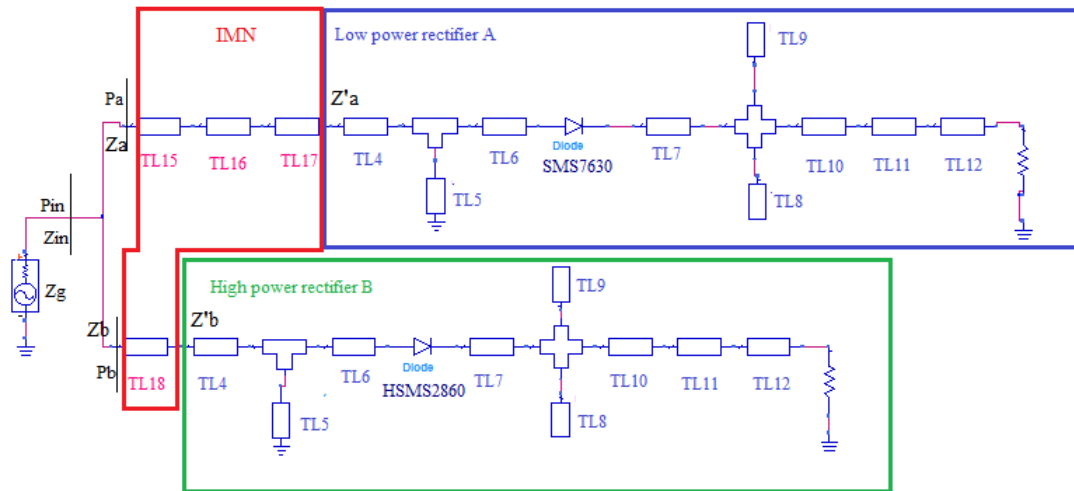
Figure 5. Schematic of the proposed wide input power range rectifier

The two subrectifiers are the same as those in previous sections. However, the impedance matching networks have been modified, and a new one has been inserted, respecting the power distribution technique. The optimized parameters of the proposed IMN are listed in Table 3. To ensure maximum PCE, the input power should be well distributed between the two subrectifiers.

Table 3. Dimensions of the proposed IMN used in the wide input power range rectifier

TL	width (mm)	length (mm)
TL15	1	9.4
TL16	4.7	8.5
TL17	4.7	2.4
TL18	7	10.4

4.2. Distribution power technique

P_{in} is the total RF input power for the array of rectifiers. P_a and P_b are the delivered powers to subrectifiers A and B, respectively. Z_{in}, Z_a, and Z_b are the input impedance of the whole system, subrectifiers A, and B, respectively. The relationship between P_{in}, P_a, and P_b can be expressed as (3) and (4):

$$P_{in} = P_a + P_b \tag{3}$$

$$\frac{P_a}{P_b} = \frac{Re(Z_b)}{Re(Z_a)} \tag{4}$$

The principle of the distribution power technique is based on the activation of one subrectifier cell based on the RF input power level and distributing the maximum of P_{in} to the considered subrectifier. At low power levels, the maximum power should be allocated to the subrectifier cell A. Thus, Z_a should match Z_g, while Z_b must be a very high impedance. Conversely, at high power, the maximum of P_{in} must be intended for subrectifier B. In this case, Z_b should match the source impedance, and subrectifier A must be deactivated, with Z_a behaving as a high impedance.

The proposed impedance matching network consists of 4 transmission lines (TL15, TL16, TL17, TL18). Three TLs (TL15, TL16, TL17) are used to match subrectifier A to 50 Ω at low input power and at high impedance at high power. Just one transmission line TL18 is used for subrectifier B to match cell B to 50 Ω at high input power and at high impedance at low power. This design allows for efficient impedance matching across varying power levels for both subrectifiers, optimizing the performance of the overall system.

Z_{15}, Z_{16}, Z_{17}, and Z_{18} are the input impedance after each transmission line. Z_{in}, Z_a, and Z_b are the input impedance of the whole system, subrectifiers A, and B, respectively. Using the transmission line theory, we can derive (5)-(8):

$$Z_{17} = Z_{TL17} \frac{Z_a' + jZ_{TL17}tan(\theta_{TL17})}{Z_{TL17} + jZ_a'tan(\theta_{TL17})} \tag{5}$$

$$Z_{16} = Z_{TL16} \frac{Z_{17} + jZ_{TL16}tan(\theta_{TL16})}{Z_{TL16} + jZ_{17}tan(\theta_{TL16})} \tag{6}$$

$$Z_a = Z_{TL15} \frac{Z_{16} + jZ_{TL15}tan(\theta_{TL15})}{Z_{TL15} + jZ_{16}tan(\theta_{TL15})} \tag{7}$$

$$Z_b = Z_{TL18} \frac{Z_b' + jZ_{TL18}tan(\theta_{TL18})}{Z_{TL18} + jZ_b'tan(\theta_{TL18})} \tag{8}$$

Besides

$$Z_{in} = Z_a || Z_b = Z_G = 50\,\Omega \tag{9}$$

$$Z_{in} = \frac{Z_a \times Z_b}{Z_a + Z_b} \tag{10}$$

In the next section, we will examine the agreement between the applied distribution technique and the simulation results.

4.3. Simulation results

The performance of the suggested wide input power range rectifier is examined in relation to the input impedance Z_{in}, reflection coefficient S_{11}, and PCE. The input impedance vs. RF input power for subrectifiers A and B are depicted in Figures 6(a) and 6(b). From these simulation results, it can be observed that there is agreement between the distribution input power technique and the behavior of the proposed rectifier.
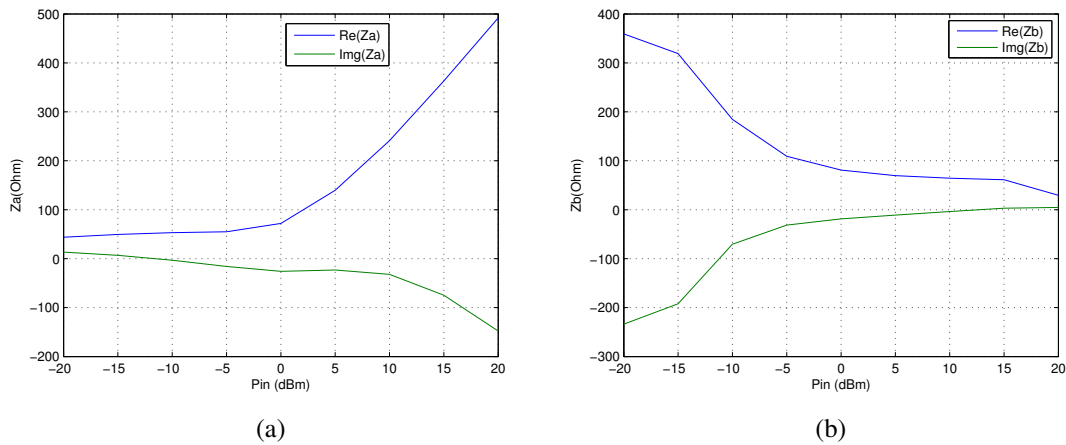
Figure 6. Simulation results (a) Z_a vs. P_{in} (b) Z_b vs. P_{in}

From -20 to 0 dBm of RF input power, Z_a is almost equal to 50 Ω, and for $P_{in} > 0$ dBm, Z_a behaves like high impedance. Conversely, the input impedance Z_b of rectifier B is practically equal to 50 Ω for P_{in} greater than 0 dBm. However, for P_{in} ranging from -20 to 0 dBm, Z_b is very high.

These results are consistent with the distribution input power technique. This approach involves allocating input power to one rectifier while deactivating the other, depending on the RF power level. Consequently, one rectifier acts as the primary energy harvester, while the other remains deactivated. This strategy ensures

efficient utilization of available RF energy and optimizes the overall performance of the system by dynamically adapting to changing power conditions.

The reflection coefficient vs. P_{in}, as illustrated in Figure 7(a), shows that rectifier A is well-matched for P_{in} from -20 to 0 dBm. On the other hand, rectifier B represents good matching for power P_{in} greater than 0 dBm, where S_{11} is always less than -10 dB. However, the designed wide input power range rectifier serves as good matching for low and high power. Figure 7(b) exhibits the power conversion efficiency vs. RF input power at 3.5 GHz. Subrectifiers A and B reach the maximum PCE at -7 dBm (35%) and 16 dBm (55%), respectively. The wide input power range rectifier represents a PCE greater than 30% over 32.5 dB (from -13 to 19.5 dBm), and it is equal to 56% and 40% at 16 and 0 dBm, respectively. It maintains $S_{11} < $ -10 dB over a 40 dB power range.
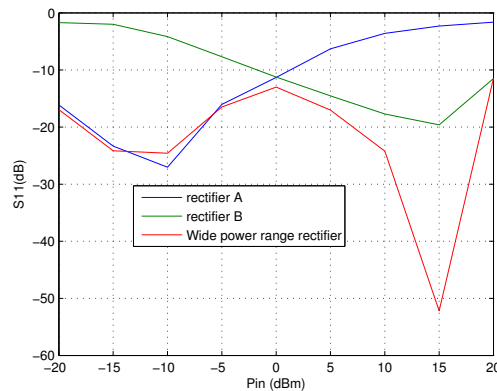
(a)
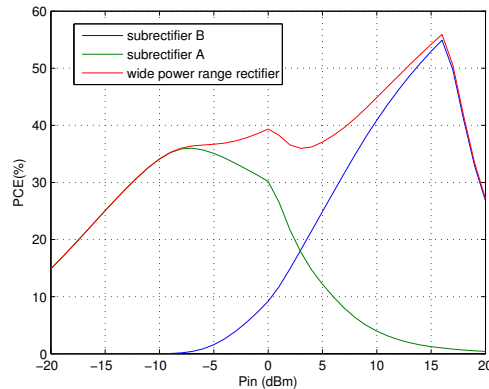
(b)

Figure 7. Simulation results (a) simulated reflection coefficient S_{11} vs. P_{in} and (b) simulated PCE vs. P_{in}

4.4. Performance comparison of the wide input power range rectifier with existing literature

To highlight the advantages of the suggested rectifying circuit, a comparative study has been carried out with existing rectifiers. The novel wide RF power band rectifier designed is dedicated for 5G applications. Utilizing microstrip-line technology without additional devices, the reduction of capacitive and inductive losses makes its implementation easier and more cost-effective compared to other rectifiers. Additionally, a simple impedance matching network composed of just three transmission lines is employed to enhance the matching between the receiving antenna and the rectifying circuit for different input power levels, spanning over 40 dB (from -20 to 20 dBm). In terms of efficiency, the studied rectifier achieves a PCE more than 30% across a 32.5 dB range of RF input power. Furthermore, after reviewing existing literature, we identified a significant gap in the designing of rectifiers operating at 3.5 GHz with a wide input power range. As far as we know, our

work is the first to address this gap by presenting a rectifier at 3.5 GHz with an wide input power range. Table 4 illustrates the results of performance comparison between the proposed rectifier and other rectifiers operating at the same sub-6 GHz band (3.5 GHz).

Table 4. Performance comparison of the rectifier with the existing literature

Ref	Year	P_{in} range for $PCE > 30\%$	PCE_{max}
[24]	2023	20dB (-5 to 15 dBm)	76% at 0 dbm
[25]	2020	–	29 % at 18 dbm
[26]	2019	–	29.7% at 6 dbm
[27]	2023	11.5 dB (-19.5 to -8 dBm)	53% at -11 dbm
[28]	2020	10 dB (-7 to 3 dBm)	43.5% at 0 dbm
[29]	2020	17 dB (-9 to 8 dBm)	66.2% at 5 dbm
[30]	2022	19 dB (-8 to 11 dB)	42.5% at 9 dbm
[31]	2020	11 dB (-7 to 4 dBm)	42% at 0 dbm
This work	2023	32.5 dB(-13 to 19.5 dBm)	56% at 16 dbm

Some rectifiers in existing literature may have a higher maximum PCE. However, it's crucial to note that our proposed rectifier excels because of its wider input power range. While some rectifiers with superior PCE might have concentrated on a narrower input power range or may not have thoroughly considered both low and high power levels. The wider input power range of our proposed rectifier makes it more versatile and applicable, enhancing its robustness as a solution.

5.   CONCLUSION

Three rectifiers designed for high, low, and wide range power levels have been proposed in this article. The high-power rectifier reached 67.4% of PCE at 15 dBm. The low-power rectifier converted 45% of RF power to DC at -2 dBm. The wide power range rectifier achieved over 32 dB of power range with a PCE greater than 30%. In the next step, these simulation results will be validated by measurement in the laboratory. An antenna operating at the 5G band will be designed and associated with rectifiers to implement a rectenna.

REFERENCES

[1]   N. A. Muhammad, N. Seman, N. I. A. Apandi, C. T. Han, Y. Li, and O. Elijah, "Stochastic geometry analysis of electromagnetic field exposure in coexisting sub-6 GHz and millimeter wave networks," *IEEE Access*, vol. 9, pp. 112780–112791, 2021, doi: 10.1109/ACCESS.2021.3103969.

[2]   T. A. Khan, A. Alkhateeb, and R. W. Heath, "Millimeter wave energy harvesting," *IEEE Transactions on Wireless Communications*, vol. 15, no. 9, pp. 6048–6062, 2016, doi: 10.1109/TWC.2016.2577582.

[3]   D. Surender, M. A. Halimi, T. Khan, F. A. Talukdar, S. K. Koul, and Y. M. M. Antar, "2.45 GHz Wi-Fi band operated circularly polarized rectenna for RF energy harvesting in smart city applications," *Journal of Electromagnetic Waves and Applications*, vol. 36, no. 3, pp. 407–423, 2022, doi: 10.1080/09205071.2021.1970030.

[4]   D. Wang, W. Chen, X. Liu, X. Li, F. M. Ghannouchi, and Z. Feng, "A 24-44 GHz broadband transmit-receive front end in 0.13-m SiGe BiCMOS for multistandard 5G applications," *IEEE Transactions on Microwave Theory and Techniques*, vol. 69, no. 7, pp. 3463–3474, 2021, doi: 10.1109/TMTT.2021.3069858.

[5]   F. Zhao, D. Inserra, G. Gao, Y. Huang, J. Li and G. Wen, "High-efficiency microwave rectifier with coupled transmission line for low-power energy harvesting and wireless power transmission," in *IEEE Transactions on Microwave Theory and Techniques*, vol. 69, no. 1, pp. 916-925, Jan. 2021, doi: 10.1109/TMTT.2020.3027011.

[6]   T. K. Nasimuddin and Y. M. M. Antar, *Elements of radio frequency energy harvesting and wireless power transfer systems*. CRC Press, 2020.

[7]   M. A. Gozel, M. Kahriman, and O. Kasar, "Design of an efficiency-enhanced Greinacher rectifier operating in the GSM 1800 band by using rat-race coupler for RF energy harvesting applications," *International Journal of RF and Microwave Computer-Aided Engineering*, vol. 29, no. 1, 2019, doi: 10.1002/mmce.21621.

[8]   P. Wu *et al.*, "Compact high-efficiency broadband rectifier with multi-stage-transmission-line matching," in *IEEE Transactions on Circuits and Systems II: Express Briefs*, vol. 66, no. 8, pp. 1316-1320, Aug. 2019, doi: 10.1109/TCSII.2018.2886432.

[9]   Y. Shi, J. Jing, Y. Fan, L. Yang, Y. Li, and M. Wang, "A novel compact broadband rectenna for ambient RF energy harvesting," *AEU - International Journal of Electronics and Communications*, vol. 95, pp. 264–270, 2018, doi: 10.1016/j.aeue.2018.08.035.

[10] T. K. Md. A Halimi M Palandoken, Yahia MM Antar, "Rectifier design challenges for WEH/WPT systems: broadening bandwidth and extending input power range," *IEEE Microwave Magazine*, 2022.

[11] I. Mansour, M. Mansour, and M. Aboualalaa, "Compact and efficient wideband rectifier based on network with wide input power ranges for energy harvesting," *AEU - International Journal of Electronics and Communications*, vol. 160, 2023, doi: 10.1016/j.aeue.2022.154516.

[12] T. Ngo, A. D. Huang, and Y. X. Guo, "Analysis and design of a reconfigurable rectifier circuit for wireless power transfer," *IEEE Transactions on Industrial Electronics*, vol. 66, no. 9, pp. 7089–7098, 2019, doi: 10.1109/TIE.2018.2875638.

[13] M. A. Halimi, D. Surender, and T. Khan, "Design of a 2.45 GHz operated rectifier with 81.5% PCE at 13 dBm input power for RFEH/WPT applications," in *2021 IEEE Indian Conference on Antennas and Propagation*, pp. 981–983, 2021, doi: 10.1109/InCAP52216.2021.9726346.

[14] D. Masotti, A. Costanzo, P. Francia, M. Filippi, and A. Romani, "A load-modulated rectifier for RF micropower harvesting with start-up strategies," *IEEE Transactions on Microwave Theory and Techniques*, vol. 62, no. 4, pp. 994–1004, 2014, doi: 10.1109/TMTT.2014.2304703.

[15] Z. X. Du and X. Y. Zhang, "High-efficiency single- and dual-band rectifiers using a complex impedance compression network for wireless power transfer," *IEEE Transactions on Industrial Electronics*, vol. 65, no. 6, pp. 5012–5022, 2018, doi: 10.1109/TIE.2017.2772203.

[16] J. Liu, X. Y. Zhang, and Q. Xue, "Dual-band transmission-line resistance compression network and its application to rectifiers," *IEEE Transactions on Circuits and Systems I: Regular Papers*, vol. 66, no. 1, pp. 119–132, 2019, doi: 10.1109/TCSI.2018.2852321.

[17] M. Huang *et al.*, "Single-and dual-band RF rectifiers with extended input power range using automatic impedance transforming, " in *IEEE Transactions on Microwave Theory and Techniques*, vol. 67, no. 5, pp. 1974-1984, May 2019, doi: 10.1109/TMTT.2019.2901443.

[18] Y. Y. Xiao, Z. X. Du, and X. Y. Zhang, "High-efficiency rectifier with wide input power range based on power recycling," *IEEE Transactions on Circuits and Systems II: Express Briefs*, vol. 65, no. 6, pp. 744–748, 2018, doi: 10.1109/TCSII.2018.2794551.

[19] J. Kim and J. Oh, "Compact rectifier array with wide input power and frequency ranges based on adaptive power distribution," *IEEE Microwave and Wireless Components Letters*, vol. 31, no. 5, pp. 513–516, 2021, doi: 10.1109/LMWC.2021.3070135.

[20] P. Wu, Y. D. Chen, W. Zhou, Z. H. Ren, and S. Y. Huang, "A wide dynamic range rectifier array based on automatic input power distribution technique," *IEEE Microwave and Wireless Components Letters*, vol. 30, no. 4, pp. 437–440, 2020, doi: 10.1109/LMWC.2020.2972727.

[21] S. A. Rotenberg, S. K. Podilchak, P. D. H. Re, C. Mateo-Segura, G. Goussetis and J. Lee, "Efficient rectifier for wireless power transmission systems, " in *IEEE Transactions on Microwave Theory and Techniques*, vol. 68, no. 5, pp. 1921-1932, May 2020, doi: 10.1109/TMTT.2020.2968055.

[22] Z. He, J. Lan, and C. Liu, "Compact rectifiers with ultra-wide input power range based on nonlinear impedance characteristics of schottky diodes," *IEEE Transactions on Power Electronics*, vol. 36, no. 7, pp. 7407–7411, 2021, doi: 10.1109/TPEL.2020.3046083.

[23] H. Ahsan, "Rectifier circuits for RF energy harvesting and wireless power transfer applications," *IEEE Sensors Journal*, pp. 46–61, 2023.

[24] M. A. Halimi, P. P. Shome, T. Khan, and S. R. Rengarajan, "Efficient single and broadband microwave rectifiers for RFEH/WPT enabled low power 5G sub-6 GHz devices," *AEU - International Journal of Electronics and Communications*, vol. 165, 2023, doi: 10.1016/j.aeue.2023.154645.

[25] S. Yoshida, K. Nishikawa, and S. Kawasaki, "C-band frequency-tunable rectifier designed by HySIC concept utilizing GaAs MMIC and Si RFIC," *IEEE Microwave and Wireless Components Letters*, vol. 30, no. 10, pp. 997–1000, 2020, doi: 10.1109/LMWC.2020.3020083.

[26] O. M. A. Dardeer, H. A. Elsadek, and E. A. Abdallah, "Compact broadband rectenna for harvesting RF energy in WLAN and WiMAX applications," in *Proceedings of 2019 International Conference on Innovative Trends in Computer Engineering*, pp. 292–296, 2019, doi: 10.1109/ITCE.2019.8646386.

[27] M. Bajtaoui, M. A. Ennasar, M. Aznabet, A. Tachrifat, and O. EL Mrabet, "A folded rectenna on a flexible substrate for 5G energy harvesting applications," *Progress In Electromagnetics Research C*, vol. 135, pp. 69–81, 2023, doi: 10.2528/PIERC23051505.

[28] A. K. M. Zakir Hossain, N. Bin Hassim, S. M. Kayser Azam, M. S. Islam, and M. K. Hasan, "A planar antenna on flexible substrate for future 5G energy harvesting in Malaysia," *International Journal of Advanced Computer Science and Applications*, vol. 11, no. 10, pp. 151–155, 2020, doi: 10.14569/IJACSA.2020.0111020.

[29] C. Bahhar, C. Baccouche, and H. Sakli, "A novel 5G rectenna for IoT applications," in *Proceedings - STA 2020: 2020 20th International Conference on Sciences and Techniques of Automatic Control and Computer Engineering*, pp. 287–290, 2020, doi: 10.1109/STA50679.2020.9329349.

[30] I. D. Bougas, M. S. Papadopoulou, A. D. Boursianis, P. Sarigiannidis, S. Nikolaidis, and S. K. Goudos, "Rectifier circuit design for 5G energy harvesting applications," in *2022 11th International Conference on Modern Circuits and Systems Technologies (MOCAST)*, Jun. 2022, pp. 1–4, doi: 10.1109/MOCAST54814.2022.9837524.

[31] S. M. K. Azam, M. S. Islam, A. K. M. Z. Hossain, and M. Othman, "Monopole antenna on transparent substrate and rectifier for energy harvesting applications in 5G," *International Journal of Advanced Computer Science and Applications*, vol. 11, no. 8, pp. 84–89, 2020, doi: 10.14569/IJACSA.2020.0110812.

BIOGRAPHIES OF AUTHORS

Mounira Ben Yamna 🆔 🔗 🆂🅲 ↻ received her engineering degree in communications and networks from National Engineering School of Gabes Tunisia in 2012, and a master degree in embedded electronics and communication systems from Higher Institute of Computer Science of Medenine Tunisia. She is currently pursuing the Ph.D. degree in electrical engineering in Systems Modeling Analysis and Control Research Laboratory, National Engineering School of Gabes Tunisia. Her works studies focused on radio frequency, energy harvesting, and antenna. She can be contacted at email: benyemnamounira@gmail.com.

Nabil Dakhli 🆔 📊 📖 ♻ received the Master degree in Electrical Engineering from Tunis University of Science, Tunisia, in 2005, and the Ph.D. degree in 2014 at the Higher School of Communication of Tunis, Tunisia. He is presently working as an Associate Professor in the Department of Electric and Computing Engineering at High Institute of Computing of Medenine, Tunisia. His current research interests include antennas, periodic structures, metamaterials and the design of RF/microwave circuits for energy harvesting and sensing. He can be contacted at email: dakhli.nabil@gmail.com.

Hedi Sakli 🆔 📊 📖 ♻ was born in Tunisia, in 1966. He received the M.S. degree in high-frequency communication systems from Marne-La-Valley University, France, in 2002, and the Ph.D. and H.D.R. degrees in telecommunications from the National Engineering School of Tunis, Tunis El-Manar University, Tunisia, in 2009 and 2014, respectively. Since 2010, he has been an Assistant Professor with the University of Gabes, where he was an Associate Professor in 2017, and Professor in 2022. He is the author of more than 140 articles. His research interests include propagation in anisotropic media, ferrite and metamaterials, numerical methods in electromagnetic, FSS, antennas, sensors, 5G, connected objects, sensor networks, and artificial intelligence. He can be contacted at email: sakli-hedi12@gmail.com.

Mohamed Aoun 🆔 📊 📖 ♻ was born in Tunisia in 1975. He graduated from National Engineering School of Gabes-Tunisia (ENIG) in 1999, and obtained his Master's and Ph.D. degrees in Automatic control from the University of Bordeaux 1 in 2000 and 2005. He is currently Professor at ENIG and member of the MACS laboratory. His research interests include system identification, robust control, fault diagnosis, set-membership approaches, fractional differentiation. He can be contacted at email: mohamed.aoun@macs.tn.